Infrared Intensities and Calculation of Infrared Band Shapes of the CO Stretching Vibrations in Substituted Tungsten Carbonyl Derivatives

CAROL L. HYDE[1] and DONALD J. DARENSBOURG*

Infrared band shapes of the carbonyl stretching vibrations in transition metal carbonyl compounds of the type *cis*-W-$(CO)_4L_2$ and *cis*-$W(CO)_4LL'$ have been calculated employing a Cauchy-Gauss product function. This technique has made it possible to assess accurately band frequencies and areas of $\nu(CO)$ in transition metal compounds. Computed band envelopes and areas are in good agreement with those measured experimentally. Infrared intensity data, obtained with the aid of band shape analyses, have been analyzed assuming that each carbonyl stretching mode exhibits a characteristic MCO group moment derivative. These results have been employed in understanding the nature of the metal–ligand bonds in compounds where L_2 = bipy, *o*-phen, tmed, diphos, arphos; L = $P(C_6H_5)_3$ and L' = NHC_5H_{10}, NC_5H_5, $C(OC_2H_5)R$ (R = CH_3, $CH_2C_6H_5$, C_6H_5); L = $As(C_6H_5)_3$ and L' = $C(OC_2H_5)CH_3$; and L = $P(OCH_2)_3CC_2H_5$ and L' = $C(OC_2H_5)CH_3$.

Introduction

Integrated infrared intensity measurements of the CO stretching vibrations in transition metal carbonyl and carbonylnitrosyl compounds have provided much information concerning the electronic character of the bonded CO group.[2-8] One of the principal experimental difficulties encountered in absolute intensity measurements for compounds containing several carbonyl groups having fairly low symmetry (*e.g.*, C_{2v}) is the problem of overlapping bands. This difficulty is particularly acute when spectra are observed in polar solvents. Quite frequently this problem is handled by simply tracing in the respective bands by hand, assuming symmetrical band shapes. However, the more extensive overlapping of the CO stretching vibrations encountered in many metal carbonyl compounds requires a more rigorous method of band separation in order to obtain meaningful infrared intensity measurements as well as accurate band frequencies.

In this paper we wish to report infrared intensity data obtained *via* band shape analyses, using Cauchy-Gauss product and/or sum functions, of the CO stretching vibrations in symmetrical and unsymmetrical substituted tungsten hexacarbonyls of the type *cis*-$W(CO)_4LL'$, where LL' = bipy, *o*-phen, tmed, diphos, arphos; L = $P(C_6H_5)_3$ and L' = NHC_5H_{10}, NC_5H_5, $C(OC_2H_5)R$ (R = CH_3, $CH_2C_6H_5$, C_6H_5); L = $As(C_6H_5)_3$ and L' = $C(OC_2H_5)CH_3$; and L = $P(OCH_2)_3CC_2H_5$ and L' = $C(OC_2H_5)CH_3$.[9] Dipole moment derivatives for the carbonyl stretching modes have been calculated from intensity measurements assuming that the four infrared-active symmetry vibrational modes each exhibit a characteristic MCO group moment derivative. The relative magnitudes of these derivatives are employed in understanding the nature of the metal-ligand bonds in these type compounds.

Experimental Section

Materials. $W(CO)_6$ was the generous gift of Climax Molybdenum Co. and was used without further purification. 4-Ethyl-2,6,7-trioxa-1-phosphabicyclo[2.2.2]octane was donated by Arapahoe Chemicals, Boulder, Colo. Organolithium and organomagnesium reagents were obtained from Alfa Products. ^{13}CO was purchased from Merck Sharp and Dohme of Canada, Ltd. Tetrahydrofuran (THF) was distilled over lithium aluminum hydride just before use. Diglyme (bis(2-methoxyethyl) ether) was refluxed over sodium and then distilled.

Preparation of Compounds. $W(CO)_4[P(C_6H_5)_3]L$, L = NHC_5H_{10} and NC_5H_5, were prepared photochemically from $W(CO)_5P(C_6H_5)_3$ and the appropriate amine by the procedure described previously.[10] $W(CO)_4L$-L (L-L = 1,10-phenanthroline (*o*-phen) and 2,2'-bipyridyl (bipy)) were prepared by the ultraviolet irradiation of a THF solution of tungsten hexacarbonyl and the corresponding amines as described by Graham and Angelici.[11] $W(CO)_4L$-L, where L-L = *N,N,N',N'*-tetramethylethylenediamine (TMED), was prepared using the procedure of Poilblanc[12] with some modifications. Tungsten hexacarbonyl was refluxed in a large excess of the amine until the calculated volume of CO was evolved. The reaction mixture was cooled and then water was added until a yellow turbid solution was obtained. The crystalline solid was collected by filtration and unreacted $W(CO)_6$ was removed by sublimation at 50° (1 mm). The product was purified by recrystallization from chloroform–methanol.

$W(CO)_4L$-L, where L-L = bis(1,2-diphenylphosphino)ethane (diphos) and 1-diphenylphosphino-2-diphenylarsinoethane (arphos), were prepared by vigorously refluxing the respective bidentate ligand and metal hexacarbonyl (in slight molar excess) in diglyme under a N_2 atmosphere until a definite color change occurred (about 75 min). The diglyme was removed under reduced pressure and unreacted $W(CO)_6$ was recovered by sublimation. The products were purified by recrystallization from chloroform–methanol.

The substituted metal tetracarbonyloxycarbenes were prepared by the method reported previously.[13]

Chemical analyses were performed by Schwarzkopf Microanalytical Laboratories, Woodside, N. Y. Analytical data and physical properties of the compounds involved in this study are given in Table I.

Infrared Measurements and Calculations. Ir spectra were recorded on a Perkin-Elmer 521 spectrophotometer in Spectrograde chloroform, *n*-hexane, or carbon disulfide. Sample concentrations were in the range 10^{-3}–10^{-4} *M*. Solutions were prepared by weighing out the solid on a Cahn electrobalance to ±0.01 mg. The solids were then added to volumetric flasks and the flasks filled accurately with solvent. Linear Beer's law plots were obtained for the $\nu(CO)$ frequencies over the absorbance range 0.15–0.75. One-millimeter matched sodium chloride cells, calibrated by the interference fringe method, were used in the measurements. The spectra were calibrated against a water va-

* To whom correspondence should be addressed at the Department of Chemistry, Tulane University, New Orleans, La. 70118.

(1) Petroleum Research Fund Fellow, 1971–1972.

(2) For an excellent review of this area see S. F. A. Kettle and I. Paul, *Advan. Organometal. Chem.*, 10, 199 (1972), and references contained therein.

(3) (a) A. Poletti, A. Foffani, and R. Cataliotti, *Spectrochim. Acta, Part A*, 26, 1063 (1969); (b) D. J. Darensbourg, *Inorg. Chim. Acta*, 4, 597 (1970).

(4) G. Keeling, S. F. A. Kettle, and I. Paul, *J. Chem. Soc. A*, 3143 (1971).

(5) D. J. Darensbourg and M. Y. Darensbourg, *Inorg. Chim. Acta*, 5, 247 (1971).

(6) W. P. Anderson and T. L. Brown, *J. Organometal. Chem.*, 32, 343 (1971).

(7) D. J. Darensbourg, *Inorg. Chem.*, 11, 1606 (1972).

(8) W. P. Anderson, T. B. Brill, A. R. Schoenberg, and C. W. Stanger, Jr., *J. Organometal. Chem.*, 44, 161 (1972).

(9) Abbreviations: bipy, 2,2'-bipyridine; *o*-phen, 1,10-phenanthroline; tmed, *N,N,N',N'*-tetramethylethylenediamine; diphos, 1,2-bis(diphenylphosphino)ethane; arphos, 1-diphenylphosphino-2-diphenylarsinoethane.

(10) G. Schwenzer, M. Y. Darensbourg, and D. J. Darensbourg, *Inorg. Chem.*, 11, 1967 (1972).

(11) J. B. Graham and R. J. Angelici, *J. Amer. Chem. Soc.*, 87, 5590 (1965).

(12) R. Poilblanc, *C. R. Acad. Sci.*, 256, 4910 (1963).

(13) C. L. Hyde and D. J. Darensbourg, *Inorg. Chim. Acta*, in press.

Table I. Analyses and Physical Properties

Compd	Mp,[a] °C	% calcd		% found		Color
		C	H	C	H	
$W(CO)_4(bipy)$	>255 dec	37.20	1.34	37.2	1.84	Dark red
$W(CO)_4(o\text{-phen})$	195 dec	40.36	1.69	40.4	1.42	Dark red
$W(CO)_4(TMED)$	>170 dec	29.14	3.91	29.7	4.22	Bright yellow
$W(CO)_4(diphos)$	199–203	51.90	3.48	51.9	3.46	Gray-white
$W(CO)_4(arphos)$	185	48.80	3.28	48.2	3.06	Green-white
$W(CO)_4(P(C_6H_5)_3)(NHC_5H_{10})$	150 dec	50.41	4.07	49.7	4.85	Yellow
$W(CO)_4(P(C_6H_5)_3)(NC_5H_5)$	145 dec	50.89	3.16	51.1	3.17	Golden
$W(CO)_4(P(C_6H_5)_3)C(OC_2H_5)CH_3$	129	49.55	3.68	49.5	3.81	Bright orange
$W(CO)_4(P(C_6H_5)_3)C(OC_2H_5)CH_2C_6H_5$	136–138	54.39	3.84	54.3	3.62	Bright orange
$W(CO)_4(P(C_6H_5)_3)C(OC_2H_5)C_6H_5$	111–114	53.78	3.64	54.0	3.56	Red-maroon
$W(CO)_4(As(C_6H_5)_3)C(OC_2H_5)CH_3$	115–116	46.32	3.44	46.4	3.43	Orange
$W(CO)_4(P(OCH_2)_3CC_2H_5)C(OC_2H_5)CH_3$	93–95	31.72	3.61	31.7	3.75	Bright yellow

[a] Melting points are uncorrected.

por spectrum below 2000 cm⁻¹ and against a CO spectrum above 2000 cm⁻¹.

The spectral slit width of the instrument was set at 1.5 cm⁻¹. The spectra were measured on an expanded abscissa scale with a scan speed of 15 cm⁻¹ min⁻¹.

Spectra for intensity measurements were recorded in absorbance and the areas under the bands were determined with a planimeter and were reproducible to at least ±1%. The base lines observed in these spectra (solvent in both cells) were linear to ±0.005 and were generally consistent with the base lines which emerged in the band-fitting process to ±0.004. Intensities were determined at a number of concentrations and extrapolated to zero concentration in order to correct for instrumental slit width effects. Data were analyzed by the linear least-squares method.

Infrared band shapes of the carbonyl stretching vibrations in the substituted metal tetracarbonyls were calculated. The analyses were carried out using a program based on the work of R. N. Jones and J. Pitha of the Division of Pure Chemistry, National Research Council of Canada.[14] The program, modified for our use, fits a Cauchy-Gauss product and/or sum function to an infrared absorption band envelope.

Force constants and the L_{ij} matrix were calculated using a modified Cotton-Kraihanzel approach developed by Jernigan, Brown, and Dobson[15] which makes no assumptions with regard to relationships among interaction constants. These calculations were performed employing a program written by Beverly Marwedel of this laboratory. For compounds for which ¹³CO frequency data were available force constant calculations were done with an iterative computer program. The four observed frequencies for the all-¹²CO species and the observed vibration for the monosubstituted, equatorial ¹³CO species were used as input in these computations. The program, based on the work of Schachtschneider and Snyder,[16] adjusts a set of force constants common to a group of related molecules.

Machine calculations were performed on a CDC 6400 at the SUNYAB Computing Center.

Results and Discussion

All of the compounds studied in this series are of the general formula $cis\text{-}W(CO)_4LL'$, where L may or may not be equivalent with L'. Hence, these compounds belong to either the C_{2v} or C_s symmetry species, respectively. In either case the infrared spectra consist of four bands corresponding to CO stretching motions. These are assigned to the two A_1, the B_1, and the B_2 modes in C_{2v} symmetry or to the two A' and two A'' modes in C_s symmetry. One of the A_1 bands (designated $A_1^{(1)}$) and the B_1 and B_2 bands are overlapped extensively (see observed spectrum in Figure 1). By the use of a Cauchy-Gauss product function it has been possible to separate these bands accurately for quantitative intensity measurements, as well as for precise frequency determinations.

The Cauchy-Gauss product function used for the calcula-

(14) R. N. Jones and J. Pitha, Bulletin No. 12, National Research Council of Canada, 1968, and references contained within.

(15) R. T. Jernigan, R. A. Brown, and G. R. Dobson, *J. Coord. Chem.*, **2**, 47 (1972).

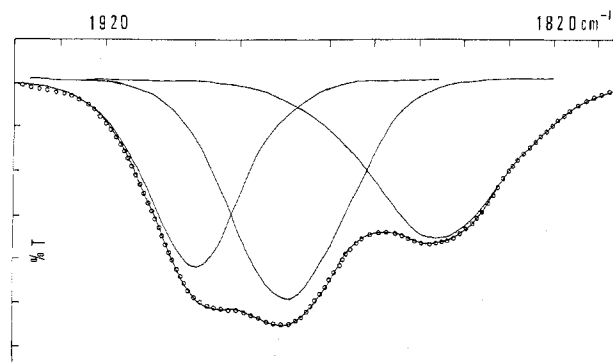(16) J. H. Schachtschneider and R. G. Snyder, *Spectrochim. Acta*, **19**, 85, 117 (1963).

Figure 1. The observed and calculated infrared band shapes in chloroform solution of $cis\text{-}W(CO)_4[P(C_6H_5)_3](NC_5H_5)$: ○, observed; –, calculated. Only the overlapping $A_1^{(1)}$, B_1, and B_2 modes are shown.

tion of the infrared band envelopes is given in the form described by Jones and Pitha (eq 1),[14] where α is the base

$$(T/T_0)_{\nu(\text{calcd})} = \exp(-2.303)\{\alpha + \sum_{P=1}^{M} \chi_{1(P)}[1 +$$
$$\chi_{3(P)}^2(\nu - \chi_{2(P)})^2]^{-1} \exp[-\chi_{4(P)}^2(\nu - \chi_{2(P)})^2]\} \quad (1)$$

line in absorbance, χ_1 is the absorbance at the band's maximum, χ_2 is the peak position in cm⁻¹, χ_3 and χ_4 together describe the half-bandwidth and the Cauchy-Gauss ratio, and M is the number of bands included in the analysis.

The band indices $(\chi_1, \chi_2, \chi_3, \chi_4)_P$ and α were varied so as to minimize φ, where

$$\phi = \sum_{\text{band}} [(T/T_0)_{\nu(\text{obsd})} - (T/T_0)_{\nu(\text{calcd})}]^2 \quad (2)$$

After the optimum band parameters were determined, the ordinates of the band envelope were calculated for each component band in both transmittance and absorbance. The areas under each band were computed using the absorbance values and Simpson's rule. In general 200–225 experimental data points taken at a constant wave number interval of 1.0 cm⁻¹ were used as input for the observed spectral comparisons. The data points used for band fitting were obtained manually and were accurate to ±0.002 transmittance unit. A representative spectrum is shown in Figure 1. Most of the calculated band shapes were closer to the Cauchy than to the Gauss shape with shape ratios, as defined by Jones and Pitha,[14] generally being greater than 0.6. A shape ratio of unity exists for a pure Cauchy band shape and a value of zero occurs for pure Gauss band shapes. The calculated band area ratios were employed in determining the absolute intensities of the overlapping symmetry vibrations. The frequencies for the compounds studied are given in Table II. Band assign-

Table II. *cis*-W(CO)$_4$LL' Infrared Band Positions (cm^{-1}) of the CO Stretching Vibrations[a]

	A$_1$$^{(2)b}$	A$_1$$^{(1)c}$	B$_1$^{c}	B$_2$^{c}
W(CO)$_4$(bipy)	2007.6	1871.5	1896.7	1826.2
W(CO)$_4$(*o*-phen)	2007.1	1871.0	1895.4	1824.0
W(CO)$_4$(TMED)	2007.8	1880.0	1861.3	1821.1
W(CO)$_4$(diphos)	2017.6	1918.5	1899.3	1873.6
W(CO)$_4$(arphos)	2018.6	1917.8	1898.0	1871.6
W(CO)$_4$(P(C$_6$H$_5$)$_3$)(NHC$_5$H$_{10}$)	2011.6	1897.5	1878.4	1837.3
W(CO)$_4$(P(C$_6$H$_5$)$_3$)(NC$_5$H$_5$)	2012.1	1901.1	1880.8	1846.7

	A$_1$$^{(2)d}$	A$_1$$^{(1)e}$	B$_2$^{e}	B$_1$^{e}
W(CO)$_4$(P(C$_6$H$_5$)$_3$)C(OC$_2$H$_5$)CH$_3$^{f}	2019.1	1925.0	1912.4	1894.9
W(CO)$_4$(P(C$_6$H$_5$)$_3$)C(OC$_2$H$_5$)C$_6$H$_5$	2021.1	1929.0	1916.7	1893.2
W(CO)$_4$(P(C$_6$H$_5$)$_3$)C(OC$_2$H$_5$)CH$_2$C$_6$H$_6$	2020.6	1928.4	1916.9	1895.3
W(CO)$_4$(As(C$_6$H$_5$)$_3$)C(OC$_2$H$_5$)CH$_3$	2020.6	1924.5	1909.8	1896.8
W(CO)$_4$(P(OCH$_2$)$_3$CC$_2$H$_5$)C(OC$_2$H$_5$)CH$_3$	2033.1	1940.7	1931.6	1912.5

^{a} The symmetry labels A$_1$$^{(2)}$ and A$_1$$^{(1)}$ correspond to A', whereas, B$_1$ and B$_2$ correspond to A'' in C_s symmetry; frequencies are accurate to 0.5 cm^{-1}. ^{b} Observed frequency in chloroform. ^{c} Frequency calculated by a Cauchy-Gauss product function, from spectra measured in chloroform. ^{d} Observed frequency in *n*-hexane. ^{e} Frequency calculated by a Cauchy-Gauss product function, from spectra measured in hexane. ^{f} The ^{13}CO frequency for one equatorially substituted species was observed at 2008.2 cm^{-1} (calculated 2006.5 cm^{-1}).

ments were made from intensity arguments.[17,18] Figure 2 shows pictorially the symmetry coordinates and their designations.

Input and output band indices for several representative compounds are given in Table III. Band fits were obtained using both product and sum functions. There was little difference in the transmittance discrepancy between observed band envelopes and those computed using either the sum or product functions. However, the product function generally led to calculated band areas which were in slightly better agreement than those obtained by the sum function. For this reason all analyses reported were obtained using the Cauchy-Gauss product function.

For several compounds the band envelopes were computed from different band input indices. These changes were as follows: frequencies were varied by ±5 cm^{-1}; peak absorbance values were varied by up to 25%; χ_3 and χ_4 indices were changed by ±0.01 to ±0.15. In all cases, the A$_1$$^{(1)}$, B$_1$, and B$_2$ frequencies were recalculated to within ±0.1 cm^{-1} of the original band positions. The per cent areas were found to deviate by a maximum of ±2.5%. The discrepancies in the transmittance differences were the same value for original and adjusted indices. This value was usually 0.3-0.4, a maximum being 0.9. From these computations, we conclude that the program output is not significantly "prejudiced" by the input indices selected.

In order to determine the intensity values of the overlapping bands, it was necessary to assume the per cent areas did not vary significantly as the sample concentration changed. Band shape analyses were done on samples of varying molar concentrations. The results for W(CO)$_4$(bipy) are summarized in Table IV which substantiate the validity of this assumption.

The measured infrared intensities of the CO stretching vi-

(17) (a) F. A. Cotton and C. S. Kraihanzel, *J. Amer. Chem. Soc.*, **84**, 4432 (1962); (b) L. E. Orgel, *Inorg. Chem.*, **1**, 25 (1962).

(18) It was possible to arrive at a satisfactory solution to the approximate CO-factored block force constant calculations by reversing the assignments of the B$_1$ and the B$_2$ modes which would simultaneously result in a reversal in the ordering of k_1 and k_2, k_1 being greater than k_2. This is analogous to the results reported previously for *cis*-Fe(CO)$_4$X$_2$ complexes by B. F. G. Johnson, J. Lewis, P. W. Robinson, and J. R. Miller, *J. Chem. Soc. A*, 1043 (1968), and I. S. Butler and H. K. Spendjian, *J. Organometal. Chem.*, **18**, 145 (1968). However, we feel strongly that the intensity arguments which dictate that the intensity of the B$_1$ mode be considerably larger than that of the B$_2$ mode are convincingly in favor of the assignment which leads to $k_2 > k_1$. Indeed, the ordering of the k_1 and k_2 force constants is one of the major consequences of being able to assess accurately the relative intensity of the B$_1$ and B$_2$ modes by band shape analysis.

Table III. Band Indices for ν_{CO} Vibrations in *cis*-W(CO)$_4$LL' Compounds

W(CO)$_4$(TMED)^a

χ_1	χ_2, cm^{-1}	χ_3	χ_4	Area, cm^{-1}
		Input		
0.322	1876.0	0.0750	0.0450	
0.303	1859.0	0.1500	0.1500	
0.219	1820.5	0.0800	0.0800	
		Output		
0.189	1880.0	0.0227	0.0963	3.398
0.239	1861.3	0.0610	0.0317	7.462
0.160	1821.1	0.0602	0.0265	5.404

$\alpha = 0.056$
The discrepancy in the transmittance differences (root mean square of $\Sigma[(T/T_0)_{\nu(obsd)} - (T/T_0)_{\nu(calcd)}]$) was found to be 0.3.

W(CO)$_4$[P(C$_6$H$_5$)$_3$](NC$_5$H$_5$)^a

χ_1	χ_2, cm^{-1}	χ_3	χ_4	Area, cm^{-1}
		Input		
0.418	1895.0	0.1000	0.1000	
0.457	1881.0	0.0500	0.0500	
0.274	1846.0	0.0600	0.0600	
		Output		
0.278	1901.1	0.0798	0.0369	6.946
0.347	1880.8	0.0476	0.0466	9.921
0.223	1846.7	0.0476	0.0284	8.391

$\alpha = 0.042$
The discrepancy in the transmittance difference (root mean square of $\Sigma[(T/T_0)_{\nu(obsd)} - (T/T_0)_{\nu(calcd)}]$) was found to be 0.4.

W(CO)$_4$[P(C$_6$H$_5$)$_3$]C(OC$_2$H$_5$)CH$_3$^{b}

χ_1	χ_2, cm^{-1}	χ_3	χ_4	Area, cm^{-1}
		Input		
0.200	1918.0	0.0500	0.0500	
0.222	1907.0	0.0600	0.0600	
0.441	1893.5	0.1000	0.1000	
		Output		
0.099	1924.9	0.0038	0.1530	1.144
0.137	1912.4	0.0224	0.0855	2.752
0.394	1894.9	0.1841	−0.0006	6.310

$\alpha = 0.044$
The discrepancy in the transmittance difference (root mean square of $\Sigma[(T/T_0)_{\nu(obsd)} - (T/T_0)_{\nu(calcd)}]$) was found to be 0.7.

^{a} Spectrum observed in chloroform solution. ^{b} Spectrum observed in hexane solution.

brations are shown in Table V. A comparison of intensity values obtained from the computed area *via* the Cauchy-Gauss product function and intensity values obtained from a least-squares plot of the experimentally measured intensity
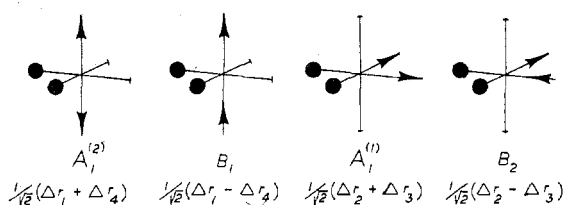
$$\frac{1}{\sqrt{2}}(\triangle r_1 + \triangle r_4) \qquad \frac{1}{\sqrt{2}}(\triangle r_1 - \triangle r_4) \qquad \frac{1}{\sqrt{2}}(\triangle r_2 + \triangle r_3) \qquad \frac{1}{\sqrt{2}}(\triangle r_2 - \triangle r_3)$$

Figure 2. Symmetry coordinates for the *cis*-W(CO)$_4$L$_2$ species. The angle between the axial carbonyl ligands is defined as 2α.

Table IV. *cis*-W(CO)$_4$(bipy) Band Shape Analysis *vs.* Concentration Study

Concn × 10³, M	ν_{CO},[a] cm⁻¹			% of area		
	B₁	A₁⁽¹⁾	B₂	B₁	A₁⁽¹⁾	B₂
1.13	1896.4	1871.1	1825.1	38.9	29.4	31.7
1.50	1896.6	1871.1	1826.0	37.1	30.2	32.6
2.16	1896.6	1871.5	1826.2	38.4	28.2	33.4

[a] Frequencies were calculated from a Cauchy–Gauss product function from spectra observed in chloroform solution.

vs. concentration has been made for several of the compounds studied. Reasonable agreement was found in most cases; results are summarized in Table VI. The calculated CO force constants and frequencies are listed in Table VII along with the L_{ij} matrix elements which are expressed in terms of symmetry coordinates.

The high-frequency (equatorial) A₁⁽²⁾ vibration involves the symmetrical stretching of trans carbonyl ligands (Figure 2). Therefore, this motion results in no net change in dipole moment derivative and consequently no intrinsic infrared intensity. However, there are three ways in which this vibration can gain intensity: (a) coupling with the A₁⁽¹⁾ axial vibration, (b) the C$_{eq}$-M-C$_{eq}$ angle departing from 180° significantly, and (c) electronic migration along the twofold axis during the stretching of the equatorial carbonyl groups.

It is possible to estimate the importance of these three factors for enhancing the intensity of the A₁⁽²⁾ vibrational mode. If coupling of the two A₁ vibrations was the sole means by which the A₁⁽²⁾ mode gains intensity, the ratio $(L_{12}/L_{22})^2$ would be directly proportional to the observed ratio of the A₁⁽²⁾ to A₁⁽¹⁾ intensities. Table VIII lists the calculated *vs.* observed A₁⁽²⁾/A₁⁽¹⁾ intensity ratios. It is clear from these comparisons that for all the compounds studied, with the lone exception of W(CO)$_4$(TMED), mixing of the two A₁ vibrational modes cannot alone account for the observed intensity of the A₁⁽²⁾ vibration.

Factor (b) can be shown to be of minor significance by calculating the contribution to the A₁⁽²⁾ intensity of a deviation in the C$_{eq}$-W-C$_{eq}$ angle of 10°. An enhancement of 2–9% is estimated based on the assumption that the A₁⁽²⁾ dipole moment derivative along the WCO bond axis is approximately the same as that observed for the A₁⁽¹⁾ derivative.[19] Crystal structure data for several related cis-disubstituted derivatives of chromium and molybdenum indicate the C$_{eq}$-M-C$_{eq}$ angle to be very close to 180°, with a minimum value of 168°.[20-23] This therefore leads to the conclusion that the sizable discrepancy between the intensity ratio as determined from a mixing of the two A₁ modes and that observed must

(19) This computation is made employing the equation, $I_{A_1}⁽²⁾ = 2G_{tt} \cos \theta (\mu_{MCO}^{A_1}{}^{(2)})$, where θ is half of the C$_{eq}$-W-C$_{eq}$ angle (170°).

(20) O. S. Mills and A. D. Redhouse, *J. Chem. Soc. A*, 1274 (1969).

(21) P. J. Roberts and J. Trotter, *J. Chem. Soc. A*, 1501 (1971).

(22) I. W. Nowell and J. Trotter, *J. Chem. Soc. A*, 2922 (1971).

(23) K. K. Cheung, T. F. Lai, and K. S. Mok, *J. Chem. Soc. A*, 1644 (1971).

be due to factor (c), an electronic migration of π charge along the twofold axis during the symmetric stretching of the equatorial carbonyl groups. The equations for calculating the magnitude of the group symmetry dipole moment derivatives are given in eq 3-6. These equations are analogous to those previously put forth for the C$_{4v}$ M(CO)$_5$L molecules,[24] where

$$I_{B_1} = 2G_{tt}\left(\mu_{MCO}^{'B_1}\right)^2 \qquad (3)$$

$$I_{B_2} = 2G_{tt} \sin^2 \alpha \left(\mu_{MCO}^{'B_2}\right)^2 \qquad (4)$$

$$I_{A_1}{}^{(2)} = \left(\sqrt{2}\mu_{MCO}^{'A_1}{}^{(2)}L_{11} + \sqrt{2}\cos\alpha \ \mu_{MCO}^{'A_1}{}^{(1)} L_{12}\right)^2 \qquad (5)$$

$$I_{A_1}{}^{(1)} = \left(\sqrt{2} \ \mu_{MCO}^{'A_1}{}^{(2)} L_{21} + \sqrt{2}\cos\alpha \ \mu_{MCO}^{'A_1}{}^{(1)} L_{22}\right)^2 \qquad (6)$$

G_{tt} equals the inverse mass of a carbonyl group (0.14585) and 2α describes the angle between axial CO groups (Figure 2). Equation 3 has sin θ = half of the C$_{eq}$-W-C$_{eq}$ angle. However, as previously mentioned θ is very close to 90° and therefore this factor is not important. It should also be noted that $\mu_{MCO}^{'A_1}{}^{(2)}$ is the net dipole moment derivative *per* carbonyl group produced by electronic charge motion perpendicular (transverse) to the equatorial carbonyl ligands.[25] This dipole moment derivative is therefore quite different from those of the other derivatives ($\mu_{MCO}^{'B_1}$, $\mu_{MCO}^{'B_2}$, and $\mu_{MCO}^{'A_1}{}^{(1)}$) which primarily involve a dipole change along the W-CO bond axis (longitudinal).

We can solve eq 5 and 6 for $\mu_{MCO}^{'A_1}{}^{(2)}$ and $\mu_{MCO}^{'A_1}{}^{(1)}$ with only a knowledge of the L_{ij} matrix elements, the angle (α), and the observed intensity values for the A₁⁽²⁾ and A₁⁽¹⁾ vibrational motions

$$\mu_{MCO}^{'A_1}{}^{(1)} = \frac{\sqrt{I_{A_1}}{}^{(2)}L_{21} - \sqrt{I_{A_1}}{}^{(1)}L_{11}}{\sqrt{2}\cos\alpha(L_{21}L_{12} - L_{11}L_{22})} \qquad (7)$$

$$\mu_{MCO}^{'A_1}{}^{(2)} = \frac{\sqrt{I_{A_1}}{}^{(2)}L_{22} - \sqrt{I_{A_1}}{}^{(1)}L_{12}}{\sqrt{2}(L_{11}L_{22} - L_{21}L_{12})} \qquad (8)$$

In calculating the A₁⁽²⁾ and A₁⁽¹⁾ dipole moment derivatives it is important to know the relative signs of $\sqrt{I_{A_1}}{}^{(2)}$ and $\sqrt{I_{A_1}}{}^{(1)}$. As shown in Figure 3 from the definition of the L_{ij} matrix elements these quantities have the same directional properties and are taken as positive quantities. Table IX lists the calculated group symmetry dipole moment derivatives.

There is a net demand made for π-electronic charge by the CO groups from the metal during the A₁⁽²⁾ and A₁⁽¹⁾ vibrational modes which is not present in the B₁ and B₂ modes. Figure 3 illustrates the relative demand for π-electronic charge made during the A₁⁽²⁾ and A₁⁽¹⁾ vibrations as indicated by the eigenvectors for the CO groups in terms of internal coordinates. As is readily seen in Figure 3, the net demand for π-electronic charge during the A₁⁽¹⁾ vibration is considerably less than that made during the A₁⁽²⁾ vibration. This is the result of extensive coupling of these symmetric vibrations and the fact that in the A₁⁽²⁾ vibration all carbonyl groups are stretching while in the A₁⁽¹⁾ vibration two carbonyl groups are stretching and two carbonyl groups are contracting. Indeed the A₁⁽¹⁾ mode makes only approxi-

(24) D. J. Darensbourg and T. L. Brown, *Inorg. Chem.*, 7, 971 (1968).

(25) This moment is analogous to the transverse component of the dipole moment gradient discussed by Kettle and coworkers.[4]

Table V. Infrared Intensities of the Carbonyl Stretching Vibrations

Compd	Intensity $\times 10^{-5}$,[a] M^{-1} cm^{-2}				
	$I_{A_1}^{(2)}$	$I_{A_1}^{(1)}$	I_{B_1}	I_{B_2}	$(I_{A_1}^{(1)} + I_{B_1} + I_{B_2})$
W(CO)$_6$[b]	7.91 ± 0.15 (7.65)				
W(CO)$_4$(TMED)[c]	0.25 ± 0.01	1.15	2.52	1.82	5.49 ± 0.11
W(CO)$_4$(bipy)[c]	0.55 ± 0.01	1.59	2.17	1.89	5.65 ± 0.19
W(CO)$_4$(o-phen)[c]	0.59 ± 0.01	1.75	2.09	1.86	5.74 ± 0.22
W(CO)$_4$(diphos)[c]	0.54 ± 0.03	0.77	2.90	1.48	5.14 ± 0.04
W(CO)$_4$(arphos)[c]	0.56 ± 0.01	0.78	3.07	1.42	5.28 ± 0.11
cis-W(CO)$_4$[P(C$_6$H$_5$)$_3$]NHC$_5$H$_{10}$[c]	0.52 ± 0.01	1.53	2.48	1.96	5.98 ± 0.11
cis-W(CO)$_4$[P(C$_6$H$_5$)$_3$]NC$_5$H$_5$[c]	0.60 ± 0.01	1.48	2.11	1.78	5.36 ± 0.07
cis-W(CO)$_4$[P(C$_6$H$_5$)$_3$]C(OC$_2$H$_5$)CH$_3$[d]	0.91 ± 0.02	0.58	3.18	1.39	5.14 ± 0.11
cis-W(CO)$_4$[(C$_6$H$_5$)$_3$]C(OC$_2$H$_5$]CH$_2$C$_6$H$_5$[d]	0.75 ± 0.01	0.81	3.08	1.42	5.31 ± 0.15
cis-W(CO)$_4$[P(C$_6$H$_5$)$_3$]C(OC$_2$H$_5$)C$_6$H$_5$[d]	0.90 ± 0.03	0.89	2.23	2.23	5.35 ± 0.19
cis-W(CO)$_4$[As(C$_6$H$_5$)$_3$]C(OC$_2$H$_5$)CH$_3$[d]	0.72 ± 0.02	0.76	2.67	1.50	4.92 ± 0.14
cis-W(CO)$_4$[P(OCH$_2$)$_3$CC$_2$H$_5$]C(OC$_2$H$_5$)CH$_3$[d]	0.79 ± 0.04	0.62	3.82	1.44	5.88 ± 0.12

[a] Errors listed are standard deviations for a least-squares plot of intensity *vs.* molar concentration plot. [b] Intensity value for the T$_{1u}$ mode in W(CO)$_6$ determined in chloroform solution; value in parentheses is in hexane solution: E. W. Abel and I. S. Butler, *Trans. Faraday Soc.*, 63, 45 (1967); K. Noack, *Helv. Chim. Acta*, 45, 1847 (1962). [c] Intensity values determined in chloroform solution. [d] Intensity values determined in hexane solution.

Table VI. Comparison of Experimental and Computed Intensity Values[a]

Compd	Concn $\times 10^4$, M	Intensity $\times 10^{-5}$, M^{-1} cm^{-2}	
		Computed	Exptl
W(CO)$_4$(TMED)	7.0	5.43	5.29 ± 0.11
W(CO)$_4$(bipy)	21.6	4.60	4.74 ± 0.20
W(CO)$_4$(diphos)	11.7	5.03	5.02 ± 0.04
W(CO)$_4$(arphos)	10.8	5.11	5.10 ± 0.11
cis-W(CO)$_4$[(C$_6$H$_5$)$_3$]NHC$_5$H$_{10}$	14.4	5.35	4.69 ± 0.11
cis-W(CO)$_4$[P(C$_6$H$_5$)$_3$]NC$_5$H$_5$	11.1	5.32	5.09 ± 0.07
cis-W(CO)$_4$[P(C$_6$H$_5$)$_3$]C(OC$_2$H$_5$)CH$_3$	5.3	4.35	4.54 ± 0.14
cis-W(CO)$_4$[As(C$_6$H$_5$)$_3$]C(OC$_2$H$_5$)CH$_3$	6.3	4.53	4.54 ± 0.14
cis-W(CO)$_4$[P(OCH$_2$)$_3$CC$_2$H$_5$]C(OC$_2$H$_5$)CH$_3$	8.3	4.52	4.32 ± 0.12

[a] Computed intensity is determined from the area calculated from the Cauchy–Gauss product function. The experimental intensity value is determined from a least-squares calculation of the intensity *vs.* concentration plot.

Table VII. Force Constants and L_{ij} Matrix Elements for the CO Stretching Vibrations

Compd	Force constants[a]					L_{ij} matrix elements	
	k_1	k_2	k_c	k_c'	k_t	$L_{12} = L_{21}$	$L_{11} = L_{22}$
W(CO)$_4$(TMED)	14.02	14.94	0.40	0.63	0.95	0.1675	0.3432
W(CO)$_4$(bipy)	13.98	15.23	0.39	0.51	0.70	0.1524	0.3502
W(CO)$_4$(o-phen)	13.90	15.28	0.33	0.47	0.77	0.1206	0.3624
W(CO)$_4$(diphos)	14.66	15.36	0.30	0.49	0.79	0.1613	0.3461
W(CO)$_4$(arphos)	14.67	15.33	0.33	0.52	0.78	0.1756	0.3391
cis-W(CO)$_4$[P(C$_6$H$_5$)$_3$]NHC$_5$H$_{10}$	14.23	15.15	0.33	0.60	0.90	0.1523	0.3502
cis-W(CO)$_4$[P(C$_6$H$_5$)$_3$]NC$_5$H$_5$	14.35	15.13	0.34	0.58	0.85	0.1699	0.3420
cis-W(CO)$_4$[P(C$_6$H$_5$)$_3$]C(OC$_2$H$_5$)CH$_3$	15.00	15.35	0.28	0.23	0.85	0.1588	0.3473
cis-W(CO)$_4$[P(C$_6$H$_5$)$_3$]C(OC$_2$H$_5$)CH$_2$C$_6$H$_5$	15.07	15.35	0.29	0.23	0.85	0.1689	0.3425
cis-W(CO)$_4$[P(C$_6$H$_5$)$_3$]C(OC$_2$H$_5$)C$_6$H$_5$	15.13	15.28	0.32	0.29	0.81	0.1998	0.3255
cis-W(CO)$_4$[As(C$_6$H$_5$)$_3$]C(OC$_2$H$_5$)CH$_3$	15.02	15.33	0.32	0.29	0.80	0.1830	0.3352
cis-W(CO)$_4$[P(OCH$_2$)$_3$CC$_2$H$_5$]C(OC$_2$H$_5$)CH$_3$	15.32	15.54	0.32	0.26	0.77	0.2128	0.3171

[a] Force constants are given in units of mdyn/Å and are defined as in ref 15.

Table VIII. Intensity Ratio Calculated from a Mixing of the A$_1$ Vibrational Modes Only

Compd	$(L_{12}/L_{22})^2$	$(I_{A_1}^{(2)}/I_{A_1}^{(1)})_{obsd}$
W(CO)$_4$(TMED)	0.24	0.22
W(CO)$_4$(bipy)	0.19	0.35
W(CO)$_4$(o-phen)	0.11	0.35
W(CO)$_4$(diphos)	0.23	0.70
W(CO)$_4$(arphos)	0.27	0.72
cis-W(CO)$_4$[P(C$_6$H$_5$)$_3$]NHC$_5$H$_{10}$	0.19	0.34
cis-W(CO)$_4$[P(C$_6$H$_5$)$_3$]NC$_5$H$_5$	0.25	0.40
cis-W(CO)$_4$[P(C$_6$H$_5$)$_3$]C(OC$_2$H$_5$)CH$_3$	0.21	1.57
cis-W(CO)$_4$[P(C$_6$H$_5$)$_3$]C(OC$_2$H$_5$)CH$_2$C$_6$H$_5$	0.24	0.93
cis-W(CO)$_4$[P(C$_6$H$_5$)$_3$]C(OC$_2$H$_5$)C$_6$H$_5$	0.38	1.01
cis-W(CO)$_4$[As(C$_6$H$_5$)$_3$]C(OC$_2$H$_5$)CH$_3$	0.30	0.95
cis-W(CO)$_4$[P(OCH$_2$)$_3$CC$_2$H$_5$]C(OC$_2$H$_5$)CH$_3$	0.45	1.27

mately a third of the demand that is made during the A$_1^{(2)}$ vibrational mode.
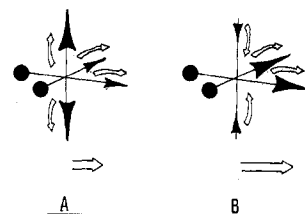

Figure 3. Electron demand for the π-electron density during the A$_1^{(2)}$ (A) and A$_1^{(1)}$ (B) motions. The magnitude of the arrows along the M–C–O bond axis represents approximately the changes in internal coordinates during these motions. The large arrows below the molecules indicate the net directions of dipole moment derivatives (or $\sqrt{I}$).

The calculated values of $\mu'^{A_1^{(2)}}_{MCO}$ reflect this demand made for π-electron density as well as the availability of π-electron density. These values are sizable for all molecules studied

Table IX. Values of μ'_{MCO}, the MCO Group Dipole Moment Derivatives[a]

Compd	$\mu'^{A_1(2)}_{MCO}$	$\mu'^{A_1(1)}_{MCO}$ [b]	$\mu'^{B_1}_{MCO}$	$\mu'^{B_2}_{MCO}$ [b]
$W(CO)_4(TMED)$	−0.12	9.80	9.29	11.17
$W(CO)_4(bipy)$	1.04	12.02	8.62	11.38
$W(CO)_4(o\text{-phen})$	1.82	12.40	8.46	11.29
$W(CO)_4(diphos)$	1.73	9.16	9.97	10.07
$W(CO)_4(arphos)$	1.52	9.34	10.26	9.87
$cis\text{-}W(CO)_4[P(C_6H_5)_3]NHC_5H_{10}$	0.98	11.77	9.22	11.59
$cis\text{-}W(CO)_4[P(C_6H_5)_3]NC_5H_5$	0.92	11.88	8.50	11.05
$cis\text{-}W(CO)_4[P(C_6H_5)_3]C(OC_2H_5)CH_3$	3.22	9.02	10.44	9.76
$cis\text{-}W(CO)_4[P(C_6H_5)_3]C(OC_2H_5)CH_2C_6H_5$	2.22	9.86	10.28	9.87
$cis\text{-}W(CO)_4[P(C_6H_5)_3]C(OC_2H_5)C_6H_5$	1.84	10.77	8.74	12.36
$cis\text{-}W(CO)_4[As(C_6H_5)_3]C(OC_2H_5)CH_3$	1.92	9.70	9.57	10.14
$cis\text{-}W(CO)_4[P(OCH_2)_3CC_2H_5]C(OC_2H_5)CH_3$	2.17	9.34	11.44	9.94

[a] The μ'_{MCO}'s are effective group dipole moment derivatives which involve both MC and CO stretching motions. The units employed here are arbitrary; the intensities are expressed in units of $10^4\ M^{-1}\ cm^{-2}$, and L and G terms are based on atomic mass units. [b] These values are calculated for $\alpha = 45°$. Crystal structure data on related compounds[20-23] indicate α values of 45–47°. Variations of this order of magnitude would change the dipole moment derivatives by less than 5%.

except for the compound containing the totally σ-bonding amine ligand (TMED). The lower values of $\mu'^{A_1(2)}_{MCO}$ are associated with the cases where only one π-bonding ligand is present ($P(C_6H_5)_3$ and amines), whereas the larger values are in turn associated with the cases where reportedly good π-bonding ligands are present (phosphines and carbenes). It is worth noting that this model for interpreting infrared intensities indicates 2,2'-bipyridine and 1,10-phenanthroline to be respectable π-bonding ligands in these tungsten(0) complexes which is consistent with the accepted behavior of these ligands toward transition metals in low oxidation states.[26]

Since the B_2 vibrational mode involves *no* net demand for electron density from the metal, it would be expected that $\mu'^{B_2}_{MCO}$ should be greater than $\mu'^{A_1(1)}_{MCO}$ for these two symmetry modes involve symmetric and asymmetric motions of the same two carbonyl ligands. However, it is possible for $\mu'^{A_1(1)}_{MCO}$ to become greater than $\mu'^{B_2}_{MCO}$ *via* π-electron migration during the $A_1^{(1)}$ stretching vibration as a result of the demand made upon the metal. From Table IV it is possible to conclude that the ratio of $\mu'^{A_1(1)}_{MCO}/\mu'^{B_2}_{MCO}$ is lowest for the complex containing the non-π-bonding TMED ligand (0.877) and is in general between 0.920 and 1.06 for the other compounds. In addition, if the uncertainty in the angle (α) is taken into account, with an upper limit of 47°, the ratio of $\mu'^{A_1(1)}_{MCO}/\mu'^{B_2}_{MCO}$ increases to 0.940–1.18. Therefore, it appears that the vibronic contribution from π-bonding ligands is slightly enhancing the intensity of the $A_1^{(1)}$ vibration.

The $\mu'^{B_2}_{MCO}$ dipole moment derivatives are expected to be larger than the $\mu'^{B_1}_{MCO}$ dipole moment derivatives if indeed the W–CO bonds trans to the substituted ligands (L and L') contain a greater degree of π-electron density as compared with those cis to the substituted ligands. $\mu'^{B_2}_{MCO}$ is in general greater than $\mu'^{B_1}_{MCO}$ with only one exception involving good π-acceptor ligands, $cis\text{-}W(CO)_4[P(OCH_2)_3CC_2H_5]C(OC_2H_5)CH_3$, where $\mu'^{B_2}_{MCO}$ is significantly less than $\mu'^{B_1}_{MCO}$.

From a comparison of the intensity (Table V) of the T_{1u} mode in $W(CO)_6$ and the total intensity of the four modes ($2\ A_1 + B_1 + B_2$) in the disubstituted tetracarbonyl derivatives an overall enhancement of intensity of $\nu(CO)$ in the latter derivatives is noted. This result is consistent with the previously reported enhancement of intensity in the monosubstituted molybdenum pentacarbonyl derivatives.[24]

It is worthwhile noting that solvent effects, such as hydrogen bonding between chloroform and the carbonyl ligand,

may affect the various symmetry vibrational modes differently. There are certainly substantial and selective solvent shifts of $\nu(CO)$ in polar solvents and, therefore, it is not unreasonable to expect some selective effects of solvent on the intensity of the various vibrational modes. Unfortunately, many of the $cis\text{-}W(CO)_4L_2$ compounds are essentially insoluble in hydrocarbon solvents, thereby eliminating a systematic testing of the nature of the solvent effect in these compounds. However, solvent effects on the intensity of $\nu(CO)$ is an interesting subject and we hope to investigate this problem for a series of compounds which are soluble in a variety of solvents. In any case, the overall view of $\nu(CO)$ intensities for the compounds involved in this study that were observed in chloroform solvent as compared to those observed in hexane is quite similar.

Conclusions

The Cauchy(Lorentz)–Gauss product or sum functions when employed in conjunction with the programs designed by Jones and Pitha[14] give very satisfactory band envelope fits for $\nu(CO)$ in transition metal carbonyl complexes. It is obvious from the preceding discussion that band shape analyses in these species provide quantitative information that is otherwise unavailable. In addition to studying infrared intensities in rather complex systems, these techniques allow for determining quantitatively the composition of mixtures of metal carbonyl species in solution.[13] These techniques should also prove useful in furnishing additional and valuable information from the infrared spectra of CO adsorbed on metal surfaces. In these cases there are frequently several closely spaced bands which are grossly overlapped.

In order to obtain meaningful results from infrared intensity measurements, which are inherently complicated quantities to determine, it is necessary to observe trends in a fairly extensive series of related compounds. From the preceding analyses of infrared intensity measurements of $\nu(CO)$ in $cis\text{-}W(CO)_4L_2$ and $cis\text{-}W(CO)_4LL'$ compounds it is possible to conclude that for the ligands bipy, o-phen, $P(C_6H_5)_3$, As-$(C_6H_5)_3$, $P(OCH_2)_3CC_2H_5$, $C(OC_2H_5)R$ ($R = CH_3$, $CH_2C_6H_5$, C_6H_5) there exists an observable metal–ligand d_π–d_π or d_π–p_π orbital occupation. This conclusion is consistent with results obtained from studies involving the above series of ligands (excluding bipy and o-phen) in monosubstituted derivatives of group VI metal carbonyls.

(26) F. A. Cotton and G. Wilkinson, "Advanced Inorganic Chemistry," 3rd ed, Interscience, New York, N. Y., 1972, p 723.

W(CO)$_4$(P(C$_6$H$_5$)$_3$)(NHC$_5$H$_{10}$), 38496-27-4; *cis*-W(CO)$_4$-(P(C$_6$H$_5$)$_3$)(NC$_5$H$_5$), 38496-28-5; *cis*-W(CO)$_4$(P(C$_6$H$_5$)$_3$)C-(OC$_2$H$_5$)CH$_3$, 38467-05-9; *cis*-W(CO)$_4$(P(C$_6$H$_5$)$_3$)C(OC$_2$H$_5$)-CH$_2$C$_6$H$_5$, 38467-06-0; *cis*-W(CO)$_4$(P(C$_6$H$_5$)$_3$)C(OC$_2$H$_5$)-C$_6$H$_5$, 38467-07-1; *cis*-W(CO)$_4$(As(C$_6$H$_5$)$_3$)C(OC$_2$H$_5$)CH$_3$, 38467-08-2; *cis*-W(CO)$_4$(P(OCH$_2$)$_3$)C(C$_2$H$_5$)C(OC$_2$H$_5$)CH$_3$, 38467-09-3.

Contribution from the Department of Chemistry, Illinois Institute of Technology, Chicago, Illinois 60616

Synthesis, Reactivity, and Spectroscopic Studies of Adducts of Isoelectronic and Isostructural Analogs of *trans*-Chlorocarbonylbis(triphenylphosphine)iridium(I) with Lewis Acids

RONALD J. FITZGERALD,*[1] NABIL Y. SAKKAB, RONALD S. STRANGE, and VYTAUTAS P. NARUTIS

Treatment of the complexes *trans*-IrCl(CO)(As(C$_6$H$_5$)$_3$)$_2$ (II), *trans*-IrCl(CS)(P(C$_6$H$_5$)$_3$)$_2$ (IV), and *trans*-IrF(CO)(P(C$_6$H$_5$)$_3$)$_2$ (V) with Lewis acids, including cyano olefins, boron halides, O$_2$, SO$_2$, and antimony halides, yields a variety of adducts. For II the O$_2$ and SO$_2$ adducts exhibit coordinated ligand reactivity. For IV the boron halide adducts undergo hydrolysis to give oxidative-addition products. A method of comparing $\Delta\bar{\nu}_{CO}$ and $\Delta\bar{\nu}_{CS}$ is advanced. On the basis of competitive reactions with the same Lewis acids, a tentative basicity order is given for II, IV, and V relative to the parent complex, *trans*-IrCl(CO)(P(C$_6$H$_5$)$_3$)$_2$ (I). Changes in $\Delta\bar{\nu}_{CO}$ and $\Delta\bar{\nu}_{CS}$ upon adduct formation are consistent with our transition metal basicity model. Limitations on this method are discussed.

Introduction

The parent complex *trans*-IrClCO(P(C$_6$H$_5$)$_3$)$_2$ (I) has been shown to undergo many diverse and interesting reactions involving oxidative addition,[2] homogeneous catalysis,[3] adduct formation with Lewis acids,[4] stabilization of molecules that do not exist at room temperature,[5] and activation of coordinated ligands.[6] Despite this extensive amount of research, the role played by the ligands in regulating the activity and basicity of complexes of type I toward Lewis acids may be of critical importance as has been indicated by recent kinetic and thermodynamic results on the rate of reversible oxygenation of metal complexes[7,8] and the activation of molecular hydrogen by metal complexes.[9]

Recently, we have become interested, in our laboratories, in investigating transition metal basicity and reactivity of metal complexes by systematically studying a group of carefully selected competitive reactions between "isostructural" and "isoelectronic" four-coordinate iridium(I) complexes and Lewis acids with a view to establish an order of relative basicity among these donors. Moreover, the strength of the interaction upon adduct formation may be estimated from the change in carbonyl stretching frequency,

$\Delta\bar{\nu}_{CO}$, upon adduct formation,[4,10] assuming that the electron density is transferred from the antibonding molecular orbital of the carbonyl moiety causing an increase in the carbonyl force constant. These results serve as a check on the competitive reactions.

Although this criterion of acid strength has worked well in general, yet one must compare the reactions of isostructural and isoelectronic metal complexes with the same Lewis acid so that if the geometry of the adduct has any influence on $\bar{\nu}_{CO}$, then the complexes will be affected in the same manner.[7,10] In addition, $\Delta\bar{\nu}$'s should not be compared for adducts and oxidative-addition reactions. In certain limited cases these data are in agreement with thermodynamic parameters for these systems.[4,11]

Experimental Section

Infrared spectra in the NaCl region were measured on a Perkin-Elmer 257 grating spectrophotometer as Nujol mulls or chloroform solutions and calibrated with polystyrene. Far-infrared spectra were recorded using a Beckman IR 11. Carbon, hydrogen, and nitrogen analyses were carried out by M-H-W Laboratories, Garden City, Mich. Sulfur analysis was done by Schwarzkopf Microanalytical Laboratory, Woodside, N. Y. Chlorine analysis was done by Dornis Kolbe Mikroanalytisches Laboratorium, Mulheim a.d. Ruhr, West Germany. Oxygen analysis was done by Micro-Tech Laboratories, Skokie, Ill.

trans-IrClCO(P(C$_6$H$_5$)$_3$)$_2$ (I) and *trans*-IrClCO(As(C$_6$H$_5$)$_3$)$_2$ (II) were purchased from Strem Chemicals, Inc., Danvers, Mass., and were used without further purification. *trans*-IrClCO(As(C$_6$H$_5$)$_3$)$_2$ was kept under nitrogen atmosphere since it reacted with atmospheric oxygen on standing. The extent of oxygen uptake is time dependent and reaches a maximum of *ca.* 20% if left indefinitely in air. To ensure the purity of the complex before performing any reaction, an infrared spectrum was recorded after heating the complex at 60° for 45 min to effect removal of any coordinated oxygen. Acrylonitrile (ACRYL), cinnamonitrile (CINNA), crotonitrile (CROTO), allyl cyanide (ALLYLCY), tetracyanoethylene (TCNE), and fumaronitrile (FUM) are Aldrich Chemical Co., Inc., products

(1) Address correspondence to the Pritzker School of Medicine, University of Chicago, Chicago, Ill. 60637.

(2) J. Halpern, *Accounts Chem. Res.*, 3, 386 (1970), and references cited therein.

(3) J. P. Collman, *Accounts Chem. Res.*, 1, 136 (1968), and references cited therein.

(4) D. F. Shriver, *Accounts Chem. Res.*, 3, 231 (1970), and references cited therein.

(5) A. P. Ginsberg and W. E. Lindsell, *J. Chem. Soc. D*, 232 (1971).

(6) J. Valentine, D. Valentine, Jr., and J. P. Collman, *Inorg. Chem.*, 10, 219 (1971).

(7) L. Vaska and S. Chen, *Chem. Commun.*, 1080 (1971).

(8) L. Vaska, S. Chen, and C. V. Senoff, *Science*, 174, 587 (1971).

(9) L. Vaska and M. F. Werneke, *Trans. N. Y. Acad. Sci.*, 33, 70 (1971).

(10) L. Vaska, *Accounts Chem. Res.*, 1, 335 (1968).

(11) L. Vaska, *Inorg. Chim. Acta*, 5, 295 (1971).